Switching between Nonisoenergetic Dynamic Covalent Reactions Using Host–Guest Chemistry

Titouan Chetot, Francesca Marocco Stuardi, Adrien Forot, Maxime Ducreux, Anne Baudouin, Emmanuel Chefdeville, Florent Perret, Laurent Vial, Julien Leclaire

Switching between Non-isoenergetic Dynamic Covalent Reactions using Host-guest Chemistry

Titouan Chetot, Francesca Marocco Stuardi, Adrien Forot, Maxime Ducreux, Anne Baudouin, Emmanuel Chefdeville, Florent Perret, Laurent Vial*, and Julien Leclaire*

Université Claude Bernard Lyon 1, CNRS, ICBMS UMR5246, CCRMN, F-69622 Villeurbanne, France.

ABSTRACT: CO_2 reacts with simple amines in presence of water to generate dynamic combinatorial libraries of majority (*i.e.*, ammonium carbamates) and minority (*i.e.*, ammonium carbonates) non-isoenergetic covalent adducts. Over the past two decades, our laboratory has reported a new class of cavitands, namely dyn[n]arenes, from which a polyanionic macrocycle is an highly efficient receptor for linear poly-ammoniums to form [2]pseudorotaxanes in water at neutral pH. Herein, we demonstrate that this formation of [2]pseudorotaxanes shifts the equilibrium of CO_2 capture by polyamines in water towards the quasi-exclusive formation of carbonate adducts, providing the first example of a switch between two competitive and reversible covalent processes triggered by host-guest interactions. In addition, this supramolecular approach to CO_2 capture exhibits enhanced capture efficiency by increasing the state of protonation of complexed *vs.* uncomplexed polyamines. Altogether, we report here that a templating approach can divert the outcome of two reversible covalent chemistries involving nucleophilic additions and acid-base reactions, challenging therefore the common knowledge that non-covalent and covalent bonds operate in separate energy frames.

INTRODUCTION

Dynamic Covalent Chemistry (DCC) is a powerful tool to generate sophisticated architectures such as macrocycles, cages, or mechanically interlocked molecules,[1–6] but also to explore complex chemical systems.[7–11] DCC relies on the self-assembly of building-blocks through dynamic covalent reactions (DCRs) to deliver Dynamic Combinatorial Libraries (DCLs), whose composition reflects the free energy of each library members.[12,13] Non-covalent binding with a template is the method of choice to selectively amplify one library member at the expense of the others.[1,5]

One of the challenges of modern DCC is to expand the chemical diversity within libraries, in terms of reactive moieties devoted either to covalent binding (building block to building block) or to non-covalent binding (building block to template). To expand the scope of covalent binding simultaneously at work within a single DCL, both orthogonal (*i.e.*, involving different reactive moieties),[14–18] and competing (*i.e.*, sharing at least one reactive moiety) DCRs were combined.[19] As covalent bonds are considered significantly more energetic than non-covalent interactions, the templating approach has only be applied so far to displace isoenergetic covalent reactions such as substitution or metathesis processes.[1,5] To the best of our knowledge, favoring one reversible covalent chemistry at the expense of another by a templating approach was never reported to date.

CO_2 capture by (poly)amines in water typically involves two competing DCRs: the carbamation and carbonation reactions.[20] In terms of mechanism, carbamation results from the nucleophilic addition of an amine on CO_2, yielding an ammonium carbamate ion pair (Figure 1i, eq. 1). Carbonation consists in the nucleophilic attack of an amine-activated water molecule on CO_2, delivering an ammonium-hydrogenocarbonate ion pair (Figure 1i, eq. 2). The ratio between carbamate and carbonate products depends on many factors, such as the CO_2 loading (*vide infra*), the Brønsted and Lewis basicity of the amine, and its dilution (*i.e.*, the amine/water stoichiometry). In the diluted millimolar concentration range, carbonation is highly favored on monoamines. If polyamines are used, the high effective molarity in nitrogen binding sites can restore the carbamation/carbonation balance.[21] The difference between the free energy of carbamation and carbonation ($\Delta\Delta_rG^\circ$) per amine site can be estimated to be around -7 kJ/mol, carbamation being enthalpically more favored than carbonation and compensated by a slightly higher entropic cost (see ESI, section II). Knowing that the free energy ($\Delta_rG°$) of a single salt bridge in water is estimated between 5 and 8 kJ/mol,[22,23] we envisioned that this non-covalent interaction may effectively shift the CO_2 capture process from carbamation to carbonation. Recently, some of us reported a new family of cyclophanes named dyn[n]arenes.[5,24–26]Among them, dyn[4]arene **1,** equipped with eight carboxylate groups, proved to be a powerful receptor for α,ω-alkyldiammonium ions in water at physiological pH. In fact, host and guests combine into [2]pseudorotaxane inclusion complexes with free energies of binding $\Delta_rG°_{binding}$ ranging from -25 to -40 kJ/mol (Figure 1ii).[5,27] The marked exergonicity of this ammonium binding event should drive the CO_2 capture process in water towards the formation of ammonium-hydrogenocarbonate ion pairs (Figure 1iii).

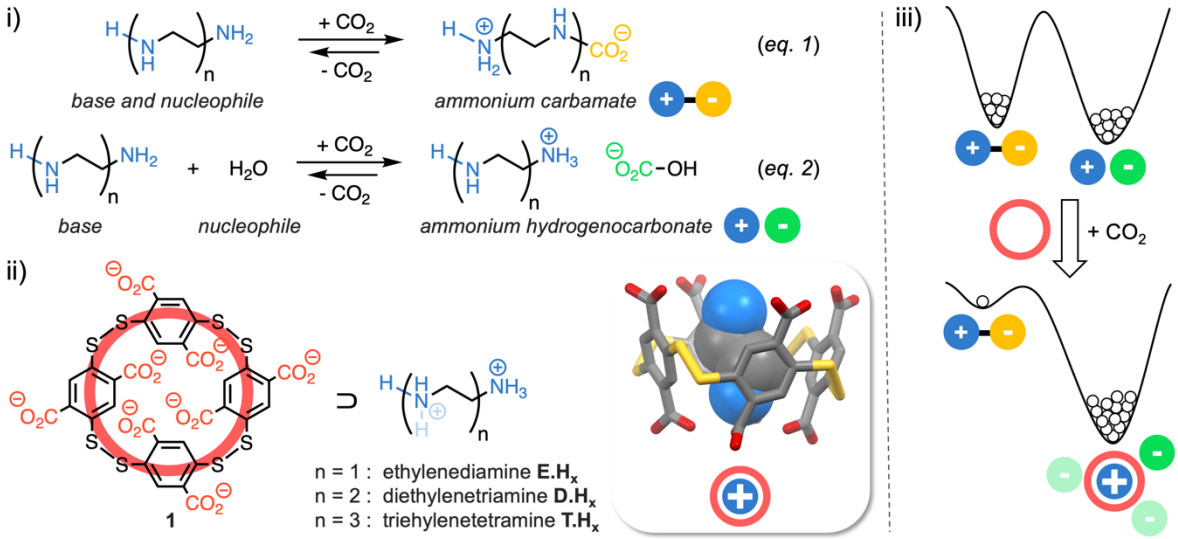

Figure 1. i) Covalent binding of CO_2 by aqueous amines: carbamation (eq. 1) and carbonation (eq. 2), ii) Dyn[4]arene **1** and its inclusion complexes with **E.H$_x$**, **D.H$_x$**, and **T.H$_x$** (computed 3D structure of **1** ⊃ **E.H$_2$** from ref. 27), and iii) expected equilibrium shift from the introduction of macrocycle **1** in non-isoenergetic DCLs of CO_2 capture by **PA** in water towards the formation of ammonium-hydrogenocarbonate ion pairs.

RESULTS AND DISCUSSION

CO_2 Capture by Poly(aminoethyl)amines. Poly(aminoethyl)amines **PA** were chosen to demonstrate the feasibility of switching the CO_2 capture covalent chemistry from carbamation to carbonation by supramolecular means.

In fact, the aminoethyl repeating unit is known to yield stable seven-membered H-bonded ammonium-carbamate rings,[28] and hence to thermodynamically favor this class of CO_2 fixation products, even in diluted medium. Ethylenediamine, the smallest member of the **PA** family, is mostly monoprotonated at physiological pH (noted **E.H$_1$**, Figure 2).[29] As such, it strongly binds to dyn[4]arene **1** ($\Delta_rG°_{binding}$ = -25.6 kJ/mol).[27] This complexation is exergonic enough to potentially counter-balance the intrinsic stability of the **E$_1$.H$_1$** ammonium carbamate zwitterion and to favor its conversion into the ammonium:hydrogenocarbonate [**E.H$_1$**:HCO_3^-] pair.[21] Higher **PA** containing two and three repeating units similarly alternate protonated and unprotonated amine groups (noted **D.H$_2$** for diethylenetriamine and **T.H$_2$** for triethylenetetramine, see Figure 2) at physiological pH.[29] ITC titrations in buffered water at $pH_0 = 7.4$ confirmed that they are even stronger guests than **E.H$_1$**, binding host **1** with an apparent free energy of -32.6 and -35.5 kJ/mol for **D.H$_2$** and **T.H$_2$**, respectively (Figure S22 and Table S2). Qualitatively, there seems to be a good correlation between the number of positive charges theoretically borne by each of the three **PA** at pH 7.4,[29] and their respective affinities with the macrocycle.[23]

Injecting a stream of CO_2 into 50 mM solutions of each **PA** (starting pH of 11.7, 12.2 and 11.7 for **E**, **D** and **T** respectively) afforded CO_2-loaded DCLs at a pH_0 of 7.4 ± 0.1 (see ESI, Section V). ^{1}H- and ^{13}C-qNMR spectroscopy analyses allowed us to identify and quantify the major library members using tetramethylphosphonium chloride as internal standard. For each library (for **D**, see Figure 3i), integration of the carbonyl signals in ^{13}C-qNMR afforded the ratio and concentrations in hydrogenocarbonate ($H\mathbf{C}O_3^-$) and carbamate (-HN-$\mathbf{C}O_2^-$) sub-libraries, hence the CO_2 loading α_N that is defined by eq. 3 as the molar ratio between CO_2 absorbed and total amount of amine moieties:

$$\alpha_N = \frac{n_i(CO_2)}{n_i(N)} \quad (eq.3)$$

, where i = **E**, **D** or **T**, $n_i(CO_2)$ is the molar amount of CO_2 bound to species i and $n_i(N)$ is the molar amount of amine groups in species i. Therefore, α_N is the average molar fraction of CO_2 bound per nitrogen binding site for each of the **PA**.

The system of ethylene multiplets (-NC**H$_2$**C**H$_2$**N-) observed in ^{1}H-qNMR splits into two sub-libraries: CO_2-bearing species (-$^+$NC**H$_2$**C**H$_2$**N$\mathbf{H}CO_2^-$) could be identified through the $^4J_{CH}$ correlation with the (-**H**N-CO_2^-) carbonyl signals, the remaining ethylene signals corresponding to the CO_2-free polyamine reservoir (for **D**, see Figure 3i). Its average protonation state was determined using the Henderson-Hasselbalch equation (Figure 2ii). This average protonation state also delivered the stoichiometry in accompanying hydrogenocarbonate counter-ions. The residual hydrogenocarbonate anions were finally assigned to the CO_2-free nitrogen centers of the CO_2-bearing (carbamate) polyamine subsystem.

From this assignment, the following compositional pictures can be provided. The untemplated DCL resulting from CO_2 capture by **E** splits into 40% of ammonium-hydrogenocarbonate ion pairs (69% of [**E.H$_1$**,HCO_3^-] and 31% of [**E.H$_2$**,2HCO_3^-]) and 60% of the **E$_1$.H$_1$** zwitterion (Figures S6-S7 and Table 1). In the case of **D**, the library is composed by two major members: the bis-hydrogenocarbonate [**D.H$_2$**,2HCO_3^-] and the mono-hydrogenocarbonate/mono-carbamate [**D$_{1s}$.H$_2$**,HCO_3^-] adduct (Figures S10-S11). In terms of absorbed CO_2, this translates into 65% of HCO_3^- and 35% of -HN-CO_2^- (Table 1).

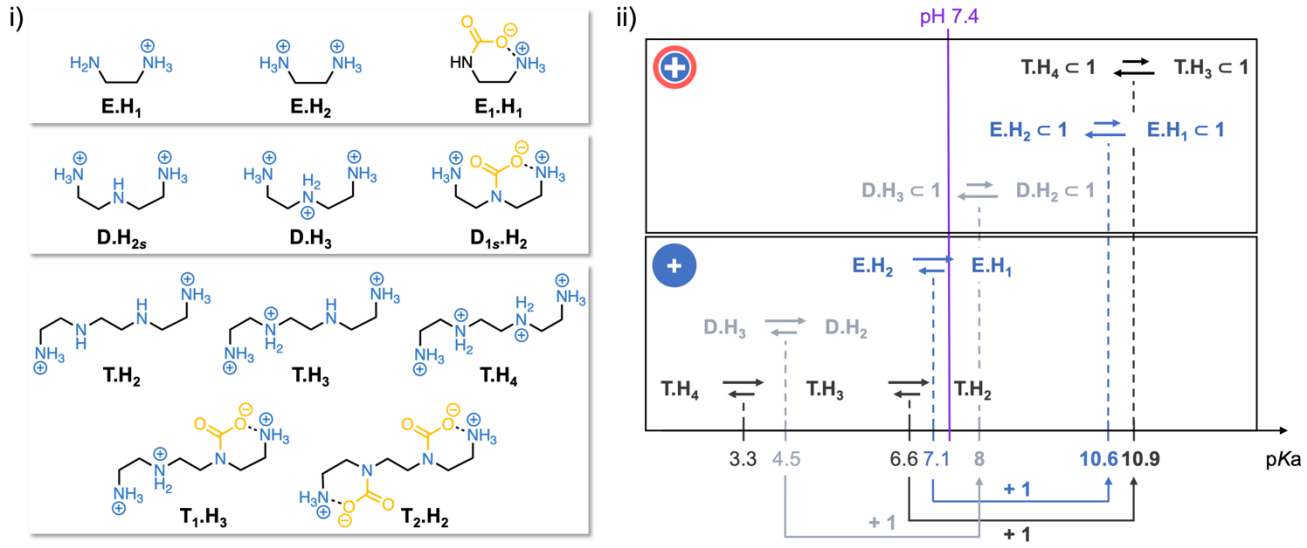

Figure 2. i) Selected members from combinatorial libraries of carbamated and/or protonated **PA** (Figure S2 and S3), and ii) pK_a values for the different protonation states of polyamines **E.H$_x$**, **D.H$_x$** and **T.H$_x$** in absence and in presence of macrocycle **1**. For comprehensive virtual combinatorial libraries of protonated and/or carbamated **E** and **D** derivatives, see Figures S2 and S3. For the sake of clarity, elements of symmetry were omitted for protonated and/or carbamated **T** derivatives.

Accurate chemical speciation of the system obtained from **T** and CO_2 was hampered by the complexity of the NMR spectra (Figures S14-S15), from which the fractions of hydrogenocarbonate (55%) HCO_3^- and carbamate -HN-CO_2^- (45%) subsystems could nevertheless be extracted (Table 1). Overall, the maximal CO_2 loading reached qualitatively mirrored the Brønsted basicity of the **PA** reactants: with average pK_a values around 8 for the -NH/-NH_2^+ and -NH_2/-NH_3^+ pairs, and 6.5 for the H_2CO_3/HCO_3^- pair, one can indeed expect CO_2-saturated solutions buffered around $pH_0 = 7.2$. Then, using the Henderson-Hasselbalch equation for each amine moiety borne by each **PA** backbone yields maximal loading values between 0.52 and 0.67, which perfectly matches our experimental data. Bottomline, the maximal loading and CO_2 capture capacity are limited by the basicity of the **PA** and more generally by the amine absorbent.

Table 1. For each DCL studied: molar fraction in hydrogenocarbonate (HCO_3^-) and carbamate (-HN-CO_2^-) moieties, and yield of CO_2 capture expressed as the loading α_N.[a]

DCL	% HCO_3^-	% -HN-CO_2^-	α_N[b]
E.H$_1$ + CO_2	40 ± 2	60 ± 4	0.55 ± 0.03
E.H$_2$ + CO_2 + **1**	85 ± 5	15 ± 1	0.88 ± 0.05
D.H$_2$ + CO_2	65 ± 4	35 ± 2	0.67 ± 0.04
D.H$_3$ + CO_2 + **1**	93 ± 6	7.0 ± 0.4	0.94 ± 0.06
T.H$_2$ + CO_2	55 ± 3	45 ± 2	0.52 ± 0.03
T.H$_4$ + CO_2 + **1**	93 ± 6	7.0 ± 0.4	0.82 ± 0.05

[a] Relative standard deviation of 6% (see ESI, Section I).

[b] Average values from the ^{1}H- and ^{13}C-qNMR analyses.

Macrocycle-induced shift of CO_2 capture chemistries by polyamines. Our previous studies reported the formation, through self-assembling in neutral water, of [2]pseudorotaxane-type complexes between α,ω-diamines or biogenic polyamines and macrocycle **1**.[5,27,30,31] Expectedly, introducing one equivalent of octacarboxylate cyclophane **1** within the DCLs generated from **PA** and CO_2 was systematically accompanied by the complexation of the polyammonium member of each library, as attested by the upfield shift of the signals corresponding to their methylene protons (for **D**, see Figure 3i; for all **PA**, see Figures S9, S13 and S17). In agreement with the amplification of the CO_2-free ammonium guests induced by this binding, the concentration of the carbamate sub-libraries dramatically decreased to levels that could not be accurately quantified by ^{13}C-qNMR (Figures S8, S12 and S16). What was less expected was the systematic pH increase ($+1.7 < \Delta pH < +2.2$) observed when mixing the mother solutions of **1** and **PA**-CO_2 DCLs, although those mother solutions were initially at a same pH of 7.4 ± 0.1. In each case, additional injection of the acid gas CO_2 (*c.a.* 0.9 equiv.) was required to reach the targeted pH of 7.4 ± 0.1. To dig deeper into the compositional modifications induced on the **PA**-CO_2 libraries by the presence of **1** (*i.e.*, beyond the proportion of carbamate and carbonate sub-libraries), detailed chemical speciation was accessed following the previous methodology (*vide supra*). Accurate quantification of the carbamate-containing species required a particular analytical effort.[32] The ^{13}C-qNMR channel provided the concentration of host-guest complexes **PA** ⊂ **1** (for **D**, see Figure 3i), which, when compared to the total amount of **PA** initially introduced, gave access to the concentration of the pool of uncomplexed guests in solution (*c.a.* 8 mM). Due to the slight difference of chemical shift ($\Delta\delta = 0.01$-0.05 ppm) and low intensity of this set of minor uncomplexed species (noted **E** ⊄ **1** or **D** ⊄ **1**) in ^{1}H-qNMR analysis, we deliberately approximated this host-free material to carbamate adducts, which is the worst case scenario in the broad context of ammonium carbonate amplification.

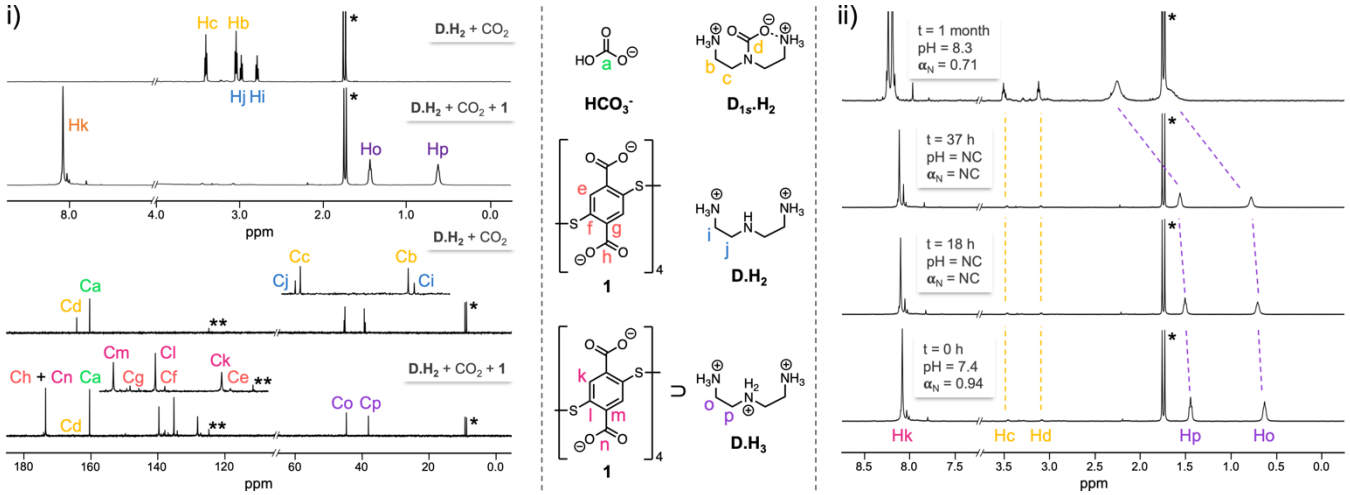

Figure 3. i) ^{1}H- and ^{13}C-qNMR spectra of aqueous CO_2-loaded solutions of **D** (50 mM, pH = 7.4) in absence or in presence of one equivalent of dyn[4]arene **1**, and ii) ^{1}H-qNMR spectra of **D** ⊂ **1** (50 mM, monitoring over time). Single asterisks indicate the signals corresponding to the internal standard (tetramethylphosphonium chloride), double asterisks indicate the signals corresponding to dissolved gaseous CO_2. NC = not calculated.

This semi-quantitative analysis led to the conclusion that dyn[4]arene **1** shifted the **E**-CO_2 and **D**-CO_2 systems toward respectively at least 85% and 93% of hydrogenocarbonate (*vs.* 15% and 7% of carbamate adducts, Table 1). Once again, the high virtual diversity of the dynamic covalent system based on **T** and CO_2 precludes the unambiguous quantification of the members of the carbamate sub-library. Mathematically, this sub-system is multivariant and cannot be solved on the sole basis of mass and charge balances, but require the quantification of a minimum set of members by spectroscopic methods. The same pessimistic approximation as for **E** ⊄ **1** and **D** ⊄ **1** was made for **T** ⊄ **1**: this share was considered to be made of a mixture of mono- or bis-carbamate adducts (**T_1.H_3** or **T_2.H_2**, Figure 2i) in undetermined proportions. If the former is the sole uncomplexed species, the amount of hydrogenocarbonate accompanying **T** ⊂ **1** would be around 95%. If the latter is the only uncomplexed species then the amount of hydrogenocarbonate accompanying the threaded ammonium drops to 91%. This provides the range of hydrogenocarbonate proportions with respect to the total amount of CO_2 absorbed in the presence of dyn[4]arene **1**, which rises from 55 to approx. 93% for **T,** similarly to **D** (Table 1 and Figure S12, S16). On the **PA** series tested, the preferential affinity displayed by host **1** for polyammoniums comparatively to ammonium carbamate guests displaced the DCRs of CO_2 capture from 42-65 % to 85-93 % of carbonation, truly inverting the fixation pathway.

Macrocycle-induced pK_a Shifts of Polyamines. As summarized in table 1, the amplification of the hydrogenocarbonate anion at the expense of carbamates is naturally accompanied by an increase in the amount of ammonium groups in the system, as well as in the maximal loading α_N reached. Both indicate that the Brønsted basicity of each **PA** is exalted by the presence of host **1**. This microscopic scenario mirrors both the pH rise (up to 9.6) observed when mixing the CO_2-saturated and neutral mother solutions of host **1** and **PA** guest, and the additional supply of CO_2 requested to bring back the templated DCL daughter samples back to pH_0 = 7.4 ± 0.1. In the case of **E** the capture yield increases by +160% with the addition of macrocycle **1**. Within the templated DCLs, the threaded guest **PA** is the only species which can potentially experience a host-induced stabilization of its conjugated acid form. In more details, the excess of CO_2 captured in the presence of receptor **1** represents between +33-36% with respect to the molar number of basic sites that are normally available on the threaded **PA**. As an example, **D** ⊂ **1** contains 137.6 mM of amine groups, 66% of which are intrinsically basic and thus eligible for carbonation (Figure S12-13). In the presence of **1** and after additional CO_2 supply to neutralize the mixture back to pH_0, a 135.3 mM concentration in hydrogenocarbonate was measured by ^{13}C-qNMR (Figure S12). This corresponds to a quantitative protonation of the entire guest backbone, including the central secondary amine site whose pK_a value is normally 4.5.

The pK_a shift of the central secondary amine of **D** induced by **1** originates from a preferential binding of the trication **DH_3** with respect to the otherwise dominant dication **DH_2**. Such pK_a shifts have previously been reported on host-guest systems, with ΔpK_a values ranging from -1.1 to +4.5 with water soluble cavitands such as cyclodextrins, sulfonatocalixarenes, or cucurbit[n]urils.[33] So far, the host-induced stabilization of protonated guest (the most explored scenario) was principally exploited for physical purposes. As solubility and emissive properties are highly related to charge density, complexation can exalt the apparent guest solubility and increase its bioavailability,[33] while controlled release from the host can be accompanied by dramatic changes in emissive properties, enabling for instance real-time enzyme activity monitoring.[34] As previously reported, pK_a shifts (ΔpK_a) can be quantified directly from the pH shifts (ΔpH) using eq. 4:

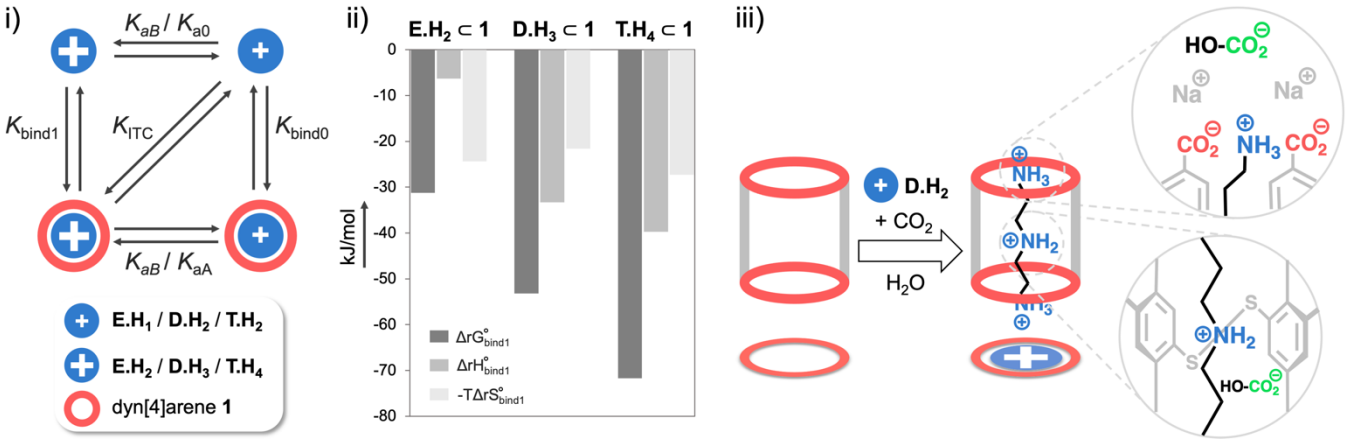

Figure 4. i) Four-state thermodynamic model from which binding constants between the different protonation states of polyamines **E.H$_x$** (x=1, 2), **D.H$_x$** (x= 2, 3) and **T.H$_4$** and dyn[4]arene **1** are extracted: K_{bind1} (or K_{bind0}) = K_{ITC} . K_{a0}/K_{aB} (or K_{a1}), where K_{ITC} is the apparent association constant measured by isothermal titration calorimetry and K_{a0} or K_{a1} are the guest acid dissociation constants in water, and K_{aB} the buffer dissociation constants in water ii) Effective Gibbs free energies, enthalpies and entropies associated to the binding of **PA** to macrocycle **1** iii) schematic representation of the formation of a [2]pseudorotaxane complex between macrocycle **1** and **D.H$_2$** to give **1** ⊃ **D.H$_3$** carrying three hydrogenocarbonate moieties.

$$\Delta pH = pH_1 - pH_0 \quad (eq.\ 4)$$

, where pH_0 and pH_1 are the pH measured in absence and in presence of macrocycle **1,** respectively. One can define a new pKa_1 for the threaded **PA** through eq. 5:

$$pH_1 = pK_{a1} + \log\left(\frac{[\mathbf{PA.H_n}\subset\mathbf{1}]}{[\mathbf{PA.H_{n+1}}\subset\mathbf{1}]}\right) \quad (eq.\ 5)$$

, which can be rewritten into eq. 6 (see ESI, section VIII for details):

$$pK_{a1} = pK_{a0} + 2\Delta pH + \log\left(\frac{C_0 - K_e * 10^{pH_0}}{C_0 - K_e * 10^{pH_1}}\right) \quad (eq.\ 6)$$

, where K_e is the water ionization constant, and C_0 is the total concentration introduced of each **PA** in solution.

In the case of **D**, a pK_a difference of +3.5 was found. It corresponds to a dramatic reversal in the **D.H$_2$/D.H$_3$** ratio, from 100/0 to up to 7/93 (Figure 2ii and S12), with the latter matching the amount of hydrogenocarbonate counterions quantified by ^{13}C-qNMR. The same behavior was observed for **E** and **T**, where the preferential non-covalent binding of dyn[4]arene **1** with their di- and tetra-protonated forms respectively provides enough Gibbs free energy (Figure 4ii, $\Delta rG°_{bind1}$) to shift the Brønsted acidity constants by 3.9 pK_a unit on average (Figure 2ii).[35] Concomitantly, this basicity enhancement by supramolecular means amplified the amount of hydrogenocarbonate which could be captured from CO_2, beyond the theoretical maximum which is otherwise dictated by the stereo-electronic features of each amine (Figure 4iii and Table 1). To put it simply, macrocycle **1** both reverses the covalent chemistry of CO_2 capture (from carbamation to carbonation) and significantly enhances the capture capacity of **PA** absorbents.

Thermodynamic Model: Protonation vs. Complexation. The selectivity displayed by neutral cavitands such as cyclodextrins, cucurbit[n]urils and pillar[n]arenes for protonated vs unprotonated guests could only be assessed so far for the most acidic *vs.* the most basic form of the latter species, by measuring the binding constants at two extreme pH values.[33] No methodology was proposed to date for non-chromophoric polyprotic guests, and this represent an analytical issue which is even more complex if the host is a polyacid such as **1**.[36] To address this open challenge, we designed a four-state thermodynamic model that is reminiscent of a double-mutant cycle,[37] from which the *effective* binding constants K_{bind0} and K_{bind1} (and their corresponding Gibbs' free energies $\Delta_rG°_{bind0}$ and $\Delta_rG°_{bind1}$) can be extracted from the *apparent* (*i.e.*, experimentally accessed) binding constants K_{ITC} (or energies $\Delta_rG°_{ITC}$) using Hess's law. Figure 4i depicts this thermodynamic cycle, which corresponds to the ITC titration experiment whose results are gathered in table S2. During this titration (diagonal of the square), two "orthogonal" elemental processes are at work: a non-covalent host-guest process (vertical vertices) and the protonation of the **PA** guest. This protonation can either occur on the free guest (top horizontal) or on the complexed guest (bottom horizontal). As the latter is more unfavorable than the former (Figure 2ii), complexation of the protonated guest is necessarily more favored than for the unprotonated guest. In practice, during the ITC titration experiment, the pH was maintained constant at 7.4 by operating in a conventional Tris buffer (*i.e.*, the Tris-H$^+$/Tris pair). In such conditions, the most abundant and most acidic species is Tris-H$^+$, which protonated both free and complexed polyamine **PA**. The latter displays a supramolecularly-enhanced basicity, with pK_{a1} values superior or equal to the pK_{aB} of Tris-H$^+$ (*c.a.* 8.1, see Table S5.)

This double decomposition of the ITC titration process can also be summarized through eq. 7 and 8 (see ESI, section X):

$$K_{\text{bind1}} = K_{ITC}\frac{K_{a0}}{K_{\text{aB}}} \quad (eq.\ 7)$$

, and:

$$K_{\text{bind0}} = K_{\text{ITC}}\frac{K_{\text{a1}}}{K_{\text{aB}}} \quad (eq.\ 8)$$

Any energy of reaction such as $\Delta_r H^\circ_{\text{bind1}}$ and $\Delta_r S^\circ_{\text{bind1}}$ can therefore be calculated from the corresponding apparent energies of binding to host **1** and the energies of protonation of the amines (See ESI, section X).

Regarding the binding constant, while K_{ITC} lie in the 10^4-10^6 range (Table S2), the K_{bind1} climb up to the 10^5-10^{12} range (Table S8). This difference clearly reveals the need to deconvolute the acid-base contribution from the experimental apparent binding values in order to truly access those of the purely non-covalent complexation process. These effective values are by far the highest ever reported for the binding of polyamines by a synthetic host in water (*i.e.*, $K_{\text{bind}} = 5.4 \times 10^{10}$ for cucurbit[6]uril with spermine),[38,39] and approach the order of magnitude of the strongest synthetic host-guest complexes involving organic partners (*i.e.*, $K_{\text{bind}} = 7.2 \times 10^{17}$ for cucurbit[7]uril with diamantane derivative).[40] This translate into Gibbs' free energies and enthalpies of **PA** ⊂ **1** complexation reaching respectively -72 and -40 kJ.mol^{-1} (Figure 4ii). These energy values of non-covalent binding events are as high as those corresponding the different covalent processes at work during CO_2 capture: proton exchange, carbonation and carbamation (see ESI, Section II and Table S8). This does not only bring the proof of our concept of switching between two CO_2 absorption chemistries by non-covalent means. It also demonstrates that host-guest processes can be a genuine driving force, displacing on demand a covalent organic reaction toward one direction (inhibition by sequestering a reactant, completion by binding the products), hence can stand as an effective synthetic tool.

Our system and the associated thermodynamic cycle displayed in Figure 4i also appear to be a valuable tool to study single molecular interactions in water. Similarly to the double mutant cycle, and as the protonation state of each species is clearly defined, this platform provides some insight on the impact of either a single protonation (**PA** vs **PA.H$^+$**) or a chain elongation (**D** vs **E**) on the energies of binding. First, it should be noted that the shift in pK_a is the direct reflection of the selectivity S of the host for the fully protonated with respect to the partially protonated guest (eq. 9 obtained as eq. 7/eq. 8, see table S7):

$$S = \frac{K_{\text{bind1}}}{K_{\text{bind0}}} = \frac{K_{\text{b1}}}{K_{\text{b0}}} = \frac{K_{\text{a0}}}{K_{\text{a1}}} \quad (eq.\ 9)$$

This selectivity factor amounts to $10^{3.5}$ per additional charge and indicates that the binding is strengthened by a factor 3000 when a supplementary proton is inserted on the **PA** backbone. This translates into a +20 kJ.mol^{-1} benefit in terms of Gibb's free energy (Figure 4ii). This value matches those reported in the literature for both cation-pi and salt-bridge interactions in polar media (both around 22.5 kJ.mol^{-1} with $\varepsilon = 25$).[41] All **PA** ⊂ **1** complexes displaying a loose binding, as attested by their substantial entropic contribution to the binding (fig 3ii), it can reasonably be assumed that whatever the guest backbone, the additional charge oscillates between the relatively non-polar aromatic walls and the highly polar carboxylate rim of **1**, hence is (on average) immersed in a relatively polar medium (for the mapping of water density in such complexes, see ref. 27). In terms of chain elongation, substituting a proton by an ethylammonium group on a primary ammonium end strengthens the binding by the same amount as the introduction of a proton on a **PA** backbone ($\Delta\Delta G^\circ$= -20 kJ.mol^{-1}). Examining entropy and enthalpy contributions confirms the loose feature of the complexes (Figure 4ii). Replacing **E.H$_2$** by **D.H$_3$** translates into a fully enthalpic benefit (additional cation-pi/anion interaction in polar medium). It also reveals that, in agreement with prior reports, this diethylenetriamino moiety corresponds to an almost optimal structural complementarity for host **1**,[27] marking the frontier between a "filling" (for guest **E**) and a "protruding" regime (for guest **T**). For the **T.H$_4$** protruding thread, optimal binding is believed to be accompanied by an oscillating shuttling movement, immersing alternatively the upper and lower diethylenetriamino core moieties into the cylindrical cavity of **1**. This explains why, further elongation of **D.H$_2$** into **T.H$_4$** principally strengthens the binding for entropic reason. Similar comparative analysis could be theoretically conducted for deprotonated **PA**. This would require assessing the enthalpy of protonation of the threaded **PA** by measuring the host-induced pH-shift discussed earlier at different temperatures. This in-depth thermodynamic investigation should be the core material for a follow-up study.

Stability of the Complexes over Time. The stability of the complexes between **1** and fully protonated/carbonated **PA** was monitored over time by ^{1}H- and ^{13}C-qNMR in aerobic condition (air headspace at room temperature, 500 ppm CO_2). Unexpectedly, in this CO_2-lean condition, the DCLs involving dyn[4]arene **1** underwent a self-consistent series of molecular events over a one-month timeframe: 1) spontaneous and slow release of the polyamines from the cavitand 2) a slight increase of the pH of the solutions, and 3) a partial release of CO_2 (Figure 3ii and S18-S20). The picture which emerges from the combination of these three elemental processes is concomitant decomplexation and deprotonation of the guest. This partial reversal of the apparent host-guest binding is believed to be due to the marked volatility of the acid used (herein CO_2). Here, the driving force is obviously the gradient in CO_2 between the rich solution and the lean headspace. Although this spontaneous slow release occurs in a CO_2-saturated unbuffered host-guest solution, the thermodynamic data from the parent ITC experiments may be examined for qualitative interpretation. Either in the presence of CO_2 or with the Tris buffer, three species (**1**, **PA**, H^+) simultaneously combine into a supramolecular complex (Fig 4iii) providing an enthalpy/entropy balance fairly different from those of conventional carbamation and carbonation process. The perturbation induced by **1** on the enthalpy/entropy balance of the CO_2 absorption processes may therefore represent a promising research direction to reduce the energy penalty required for CO_2 stripping and absorbent regeneration. Moreover, in contrast to conventional cavitands, host **1** is a constitutionally dynamic species. Its controlled self-

assembling from/dissociation into the starting monomeric building block may thus provide a complementary and powerful strategy to trigger CO_2 absorption/desorption and partial **PA** protonation/deprotonation thus offering a supramolecular assisted CO_2 capture cycle. We are currently testing these scenarios, and results will be reported in due course.

CONCLUSIONS

In conclusion, we described the first supramolecular switch between reversible covalent processes, where host-guest chemistry can not only shift the covalent equilibria of CO_2 capture by polyamines towards the exclusive formation of carbonate adducts, but also increase CO_2 capture efficiency by polyamines. This synergetic outcome was explained by the highly favorable formation of inclusion complexes between an polyanionic dyn[4]arene and fully protonated polyamines. This supramolecular binding event not only provides enough energy to counter-balance the gap between the two non-isoenergetic CO_2 capture chemistries, but also to induce pK_a shifts on polyamine guests, thereby increasing their net charge and CO_2 loading beyond the theoretical limit. Interestingly, these pK_a shifts induced by the formation of [2]pseudorotaxane-type complexes are in the same order of magnitude as those observed in biogenic macromolecules such as proteins ($-6.6 < \Delta pK_a < +5.7$), where the microenvironment perturbs the intrinsic pK_a of their constituting amino acids.[42,43] Here we provided an accompanying framework under the form of a double mutant (protonation *vs*. complexation) cycle, which allows the user to deconvolute acid-base from non-covalent binding when polyacidic species are involved. This conceptual tool not only provides access to the energetic features of each elementary step, but also allows to assess the energetic impact of punctual structural changes (from protonation to chain elongation) on the binding. This straightforward structure-activity relating tool should therefore effectively assist the design of powerful host-guest systems in water. Altogether, we report here that a templating approach can divert the outcome of two reversible covalent chemistries involving nucleophilic additions and acid-base reactions, challenging therefore the common knowledge that non-covalent and covalent bonds operate in separate energy frames. Capture processes based on host-induced CO_2 loading and release may illustrate in the future the added value of non-covalent events into separative processes.

ASSOCIATED CONTENT

Supporting Information.
General methods, thermodynamic models, sample preparation, ^{1}H- and ^{13}C-qNMR analyses, ITC experiments, and X-ray crystallography.

AUTHOR INFORMATION

Corresponding Author

* laurent.vial@univ-lyon1.fr, julien.leclaire@univ-lyon1.fr

Funding Sources

Financial support from the French MESR (T.C., F.M.S. and M.D.), from MeCaWaRe SAS (M.D.), and the ADEME (A.F.) is gratefully acknowledged. This work was supported by the LABEX iMUST (ANR-10-LABX-0064) of Université de Lyon, within the program "Investissements d'Avenir" operated by the French National Research Agency (ANR).

ACKNOWLEDGMENT

We thank the IBCP and CCRMN for assistance with ITC and NMR analyses, respectively. The authors are very grateful to Prof. I. Huc and Dr P. K. Mandal for crystal growing, data collection, and crystal refinement.

REFERENCES

(1) Shen, L.; Cao, N.; Tong, L.; Zhang, X.; Wu, G.; Jiao, T.; Yin, Q.; Zhu, J.; Pan, Y.; Li, H. Dynamic Covalent Self-Assembly Based on Oxime Condensation. *Angew Chem Int Ed* **2018**, *57* (50), 16486–16490. https://doi.org/10.1002/anie.201811025.

(2) Kołodziejski, M.; Stefankiewicz, A. R.; Lehn, J.-M. Dynamic Polyimine Macrobicyclic Cryptands – Self-Sorting with Component Selection. *Chem. Sci.* **2019**, *10* (6), 1836–1843. https://doi.org/10.1039/C8SC04598D.

(3) Gianga, T.-M.; Audibert, E.; Trandafir, A.; Kociok-Köhn, G.; Pantoş, G. D. Discovery of an All-Donor Aromatic [2]Catenane. *Chem. Sci.* **2020**, *11* (35), 9685–9690. https://doi.org/10.1039/D0SC04317F.

(4) Schröder, H. V.; Zhang, Y.; Link, A. J. Dynamic Covalent Self-Assembly of Mechanically Interlocked Molecules Solely Made from Peptides. *Nat. Chem.* **2021**, *13* (9), 850–857. https://doi.org/10.1038/s41557-021-00770-7.

(5) Skowron, P.-T.; Dumartin, M.; Jeamet, E.; Perret, F.; Gourlaouen, C.; Baudouin, A.; Fenet, B.; Naubron, J.-V.; Fotiadu, F.; Vial, L.; Leclaire, J. On-Demand Cyclophanes: Substituent-Directed Self-Assembling, Folding, and Binding. *J. Org. Chem.* **2016**, *81* (2), 654–661. https://doi.org/10.1021/acs.joc.5b02605.

(6) Ponnuswamy, N.; Cougnon, F. B. L.; Pantoş, G. D.; Sanders, J. K. M. Homochiral and *Meso* Figure Eight Knots and a Solomon Link. *J. Am. Chem. Soc.* **2014**, *136* (23), 8243–8251. https://doi.org/10.1021/ja4125884.

(7) Vantomme, G.; Jiang, S.; Lehn, J.-M. Adaptation in Constitutional Dynamic Libraries and Networks, Switching between Orthogonal Metalloselection and Photoselection Processes. *J. Am. Chem. Soc.* **2014**, *136* (26), 9509–9518. https://doi.org/10.1021/ja504813r.

(8) Gu, R.; Lehn, J.-M. Constitutional Dynamic Selection at Low Reynolds Number in a Triple Dynamic System: Covalent Dynamic Adaptation Driven by Double Supramolecular Self-Assembly. *J. Am. Chem. Soc.* **2021**, *143* (35), 14136–14146. https://doi.org/10.1021/jacs.1c04446.

(9) Yang, Z.; Lehn, J.-M. Dynamic Covalent Self-Sorting and Kinetic Switching Processes in Two Cyclic Orders: Macrocycles and Macrobicyclic Cages. *J. Am. Chem. Soc.* **2020**, *142* (35), 15137–15145. https://doi.org/10.1021/jacs.0c07131.

(10) Yang, S.; Geiger, Y.; Geerts, M.; Eleveld, M. J.; Kiani, A.; Otto, S. Enantioselective Self-Replicators. *J. Am. Chem. Soc.* **2023**, *145* (30), 16889–16898. https://doi.org/10.1021/jacs.3c05472.

(11) Liu, K.; Blokhuis, A.; Van Ewijk, C.; Kiani, A.; Wu, J.; Roos, W. H.; Otto, S. Light-Driven Eco-Evolutionary Dynamics in a Synthetic Replicator System. *Nat. Chem.* **2024**, *16* (1), 79–88. https://doi.org/10.1038/s41557-023-01301-2.

(12) Corbett, P. T.; Leclaire, J.; Vial, L.; West, K. R.; Wietor, J.-L.; Sanders, J. K. M.; Otto, S. Dynamic Combinatorial Chemistry. *Chem. Rev.* **2006**, *106* (9), 3652–3711. https://doi.org/10.1021/cr020452p.

(13) Orrillo, A. G.; Furlan, R. L. E. Sulfur in Dynamic Covalent Chemistry. *Angew Chem Int Ed* **2022**, *61* (26), e202201168. https://doi.org/10.1002/anie.202201168.

(14) Zhang, K.; Matile, S. Complex Functional Systems with Three Different Types of Dynamic Covalent Bonds. *Angew Chem Int Ed* **2015**, *54* (31), 8980–8983. https://doi.org/10.1002/anie.201503033.

(15) Drożdż, W.; Walczak, A.; Stefankiewicz, A. R. Simultaneous Formation of a Fully Organic Triply Dynamic Combinatorial Library. *Org. Lett.* **2021**, *23* (9), 3641–3645. https://doi.org/10.1021/acs.orglett.1c01042.

(16) Marić, I.; Yang, L.; Li, X.; Santiago, G. M.; Pappas, C. G.; Qiu, X.; Dijksman, J. A.; Mikhailov, K.; Van Rijn, P.; Otto, S. Tailorable and Biocompatible Supramolecular-Based Hydrogels Featuring Two Dynamic Covalent Chemistries. *Angew Chem Int Ed* **2023**, *62* (14), e202216475. https://doi.org/10.1002/anie.202216475.

(17) Stefankiewicz, A. R.; Sambrook, M. R.; Sanders, J. K. M. Template-Directed Synthesis of Multi-Component Organic Cages in Water. *Chem. Sci.* **2012**, *3* (7), 2326. https://doi.org/10.1039/c2sc20347b.

(18) Reuther, J. F.; Dahlhauser, S. D.; Anslyn, E. V. Tunable Orthogonal Reversible Covalent (TORC) Bonds: Dynamic Chemical Control over Molecular Assembly. *Angew Chem Int Ed* **2019**, *58* (1), 74–85. https://doi.org/10.1002/anie.201808371.

(19) Leclaire, J.; Vial, L.; Otto, S.; Sanders, J. K. M. Expanding Diversity in Dynamic Combinatorial Libraries: Simultaneous Exchange of Disulfide and Thioester Linkages. *Chem. Commun.* **2005**, No. 15, 1959. https://doi.org/10.1039/b500638d.

(20) Septavaux, J.; Tosi, C.; Jame, P.; Nervi, C.; Gobetto, R.; Leclaire, J. Simultaneous CO2 Capture and Metal Purification from Waste Streams Using Triple-Level Dynamic Combinatorial Chemistry. *Nat. Chem.* **2020**, *12* (2), 202–212. https://doi.org/10.1038/s41557-019-0388-5.

(21) Ducreux, M.; Tosi, C.; Stuardi, F. M.; Septavaux, J. The Need for a Systemic and Standardized Approach in CO2 Capture.

(22) Kubik, S. When Molecules Meet in Water-Recent Contributions of Supramolecular Chemistry to the Understanding of Molecular Recognition Processes in Water. *ChemistryOpen* **2022**, *11* (4), e202200028. https://doi.org/10.1002/open.202200028.

(23) Biedermann, F.; Schneider, H.-J. Experimental Binding Energies in Supramolecular Complexes. *Chem. Rev.* **2016**, *116* (9), 5216–5300. https://doi.org/10.1021/acs.chemrev.5b00583.

(24) Donnier-Maréchal, M.; Septavaux, J.; Jeamet, E.; Héloin, A.; Perret, F.; Dumont, E.; Rossi, J.-C.; Ziarelli, F.; Leclaire, J.; Vial, L. Diastereoselective Synthesis of a Dyn[3]Arene with Distinct Binding Behaviors toward Linear Biogenic Polyamines. *Org. Lett.* **2018**, *20* (8), 2420–2423. https://doi.org/10.1021/acs.orglett.8b00766.

(25) Vial, L.; Perret, F.; Leclaire, J. Dyn[*n*]Arenes: Versatile Platforms To Study the Interplay between Covalent and Noncovalent Bonds. *Eur J Org Chem* **2022**, *2022* (2), e202101274. https://doi.org/10.1002/ejoc.202101274.

(26) Zhang, Y.; Ourri, B.; Skowron, P.-T.; Jeamet, E.; Chetot, T.; Duchamp, C.; Belenguer, A. M.; Vanthuyne, N.; Cala, O.; Dumont, E.; Mandal, P. K.; Huc, I.; Perret, F.; Vial, L.; Leclaire, J. Self-Assembly of Achiral Building Blocks into Chiral Cyclophanes Using Non-Directional Interactions. *Chem. Sci.* **2023**, *14* (26), 7126–7135. https://doi.org/10.1039/D3SC01235B.

(27) Jeamet, E.; Septavaux, J.; Héloin, A.; Donnier-Maréchal, M.; Dumartin, M.; Ourri, B.; Mandal, P.; Huc, I.; Bignon, E.; Dumont, E.; Morell, C.; Francoia, J.-P.; Perret, F.; Vial, L.; Leclaire, J. Wetting the Lock and Key Enthalpically Favours Polyelectrolyte Binding. *Chem. Sci.* **2019**, *10* (1), 277–283. https://doi.org/10.1039/C8SC02966K.

(28) Said, R. B.; Kolle, J. M.; Essalah, K.; Tangour, B.; Sayari, A. A Unified Approach to CO2–Amine Reaction Mechanisms. *ACS*

Omega **2020**, *5* (40), 26125-26133. https://doi.org/10.1021/acsomega.0c03727.

(29) Smith, R. M.; Martell, A. E. *Critical Stability Constants*; Springer US: Boston, MA, 1975. https://doi.org/10.1007/978-1-4613-4452-0.

(30) Vial, L.; Ludlow, R. F.; Leclaire, J.; Pérez-Fernández, R.; Otto, S. Controlling the Biological Effects of Spermine Using a Synthetic Receptor. *J. Am. Chem. Soc.* **2006**, *128* (31), 10253–10257. https://doi.org/10.1021/ja062536b.

(31) For a crystal structure of uncomplexed **1**, see Figure S21. The structure highlights the propensity of the macrocycle to interact with sodium cations, which may have a significant impact on its affinity with polyamines, see: Gómez-González, B.; Basílio, N.; Vaz, B.; Pérez-Lorenzo, M.; García-Río, L. Delving into the Variability of Supramolecular Affinity: Self-Ion Pairing as a Central Player in Aqueous Host-Guest Chemistry. *Angew. Chem. Int. Ed.* **2024**, 63, e202317553. https:// doi/10.1002/anie.202317553.

(32) First, we evaluated the amount of hydrogenocarbonate ions (*i.e.,* 12 mM) generated upon CO_2 bubbling through a 50 mM solution of dyn[4]arene **1** in water as a blank experiment (see ESI, Section VI), allowing us to quantified the actual contribution of polyamines to CO_2 capture.

(33) Ghosh, I.; Nau, W. M. The Strategic Use of Supramolecular pKa Shifts to Enhance the Bioavailability of Drugs. *Advanced Drug Delivery Reviews* **2012**, *64* (9), 764–783. https://doi.org/10.1016/j.addr.2012.01.015.

(34) Praetorius, A.; Bailey, D. M.; Schwarzlose, T.; Nau, W. M. Design of a Fluorescent Dye for Indicator Displacement from Cucurbiturils: A Macrocycle-Responsive Fluorescent Switch Operating through a p K_a Shift. *Org. Lett.* **2008**, *10* (18), 4089–4092. https://doi.org/10.1021/ol8016275.

(35) We demonstrated that, in presence of macrocycle **1**, polyammoniums **TETA.H$_3$** and **TETA.H$_4$** are the dominant species at pH 7.4 (see ESI section VIII).

(36) Shaikh, M.; Dutta Choudhury, S.; Mohanty, J.; Bhasikuttan, A. C.; Nau, W. M.; Pal, H. Modulation of Excited-State Proton Transfer of 2-(2′-Hydroxyphenyl)Benzimidazole in a Macrocyclic Cucurbit[7]Uril Host Cavity: Dual Emission Behavior and p K_a Shift. *Chemistry A European J* **2009**, *15* (45), 12362–12370. https://doi.org/10.1002/chem.200900390.

(37) Cockroft, S. L.; Hunter, C. A. Chemical Double-Mutant Cycles: Dissecting Non-Covalent Interactions. *Chem. Soc. Rev.* **2007**, *36* (2), 172–188. https://doi.org/10.1039/B603842P.

(38) Barrow, S. J.; Kasera, S.; Rowland, M. J.; Del Barrio, J.; Scherman, O. A. Cucurbituril-Based Molecular Recognition. *Chem. Rev.* **2015**, *115* (22), 12320–12406. https://doi.org/10.1021/acs.chemrev.5b00341.

(39) Rekharsky, M. V.; Mori, T.; Yang, C.; Ko, Y. H.; Selvapalam, N.; Kim, H.; Sobransingh, D.; Kaifer, A. E.; Liu, S.; Isaacs, L.; Chen, W.; Moghaddam, S.; Gilson, M. K.; Kim, K.; Inoue, Y. A Synthetic Host-Guest System Achieves Avidin-Biotin Affinity by Overcoming Enthalpy–Entropy Compensation. *Proc. Natl. Acad. Sci. U.S.A.* **2007**, *104* (52), 20737–20742. https://doi.org/10.1073/pnas.0706407105.

(40) Cao, L.; Šekutor, M.; Zavalij, P. Y.; Mlinarić-Majerski, K.; Glaser, R.; Isaacs, L. Cucurbit[7]uril·Guest Pair with an Attomolar Dissociation Constant. *Angew Chem Int Ed* **2014**, *53* (4), 988–993. https://doi.org/10.1002/anie.201309635.

(41) Gallivan, J. P.; Dougherty, D. A. A Computational Study of Cation−π Interactions vs Salt Bridges in Aqueous Media: Implications for Protein Engineering. *J. Am. Chem. Soc.* **2000**, *122* (5), 870–874. https://doi.org/10.1021/ja991755c.

(42) Isom, D. G.; Castañeda, C. A.; Cannon, B. R.; García-Moreno E., B. Large Shifts in pK $_a$ Values of Lysine Residues Buried inside a Protein. *Proc. Natl. Acad. Sci. U.S.A.* **2011**, *108* (13), 5260–5265. https://doi.org/10.1073/pnas.1010750108.

(43) Harris, T. K.; Turner, G. J. Structural Basis of Perturbed pKa Values of Catalytic Groups in Enzyme Active Sites. *IUBMB Life* **2002**, *53* (2), 85–98. https://doi.org/10.1080/15216540211468.